Article

Determining the Surface pK_a of Perfluorooctanoic Acid

Lila J. Musegades, Owen P. Curtin, and Jenée D. Cyran*

Read Online

ACCESS | Metrics & More | Article Recommendations

ABSTRACT: Perfluorooctanoic acid (PFOA) is an environmentally prevalent and persistent organic pollutant with toxic and bioaccumulative properties. Despite the known importance of perfluorinated pollutants in the global environment, molecular-level details of the physicochemical behavior of PFOA on aqueous interfaces remain poorly understood. Here, we utilized two surface-specific techniques, vibrational sum frequency generation spectroscopy (SFG) and surface tensiometry, to investigate the pH-induced structural changes of PFOA and octanoic acid (OA) and determined the apparent pK_a at the air−water surface. The SFG spectra and surface activity model were investigated over a wide range of pHs. With the surface tension measurements, the surface pK_a values for OA and PFOA are determined to be 3.8 ± 0.1 and 2.2 ± 0.2, respectively. These results could provide insights into improved remediation of PFOAs and may impact climate modeling of perfluorinated alkyl chain molecules.
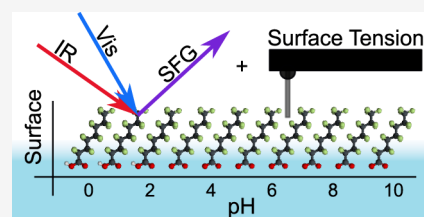
1. INTRODUCTION

Perfluorooctanoic acid (PFOA) is a man-made surfactant with a fluorinated alkyl tail and is detected in the natural environment, homes, and offices.[1] PFOA and other per- and polyfluorinated alkyl substances (PFAS) have been produced for over 60 years for firefighting foams, biomedical applications, food preservation, cosmetics, water- or stain-resistant coatings, and inert materials.[2−5] Thin films or coatings of these versatile chemicals impart the material with the desirable properties of PFAS: the high structural stability, hydrophobicity, low adhesion, high hydrophobicity, and heat resistance.[6] However, the widespread usage and lack of natural degradation pathways led to an accumulation of PFAS in the environment and the classification of PFAS as persistent organic pollutants.[7] PFAS have been linked to several notable health issues, including carcinogenic properties and bioaccumulation damaging the kidney, thyroid, and reproductive health.[8−12]

Numerous studies have investigated various properties of PFOA to better understand the thorough dispersion throughout ecological systems. However, there are numerous interpretations of the bulk pK_a reported in the literature from several separate techniques. The interpretations vary over a wide range of pHs from 0 to 3.8 and some papers discussing the difficulties of experimentally studying the fluorinated chains with 6−8 carbons.[13−15]

The fluorines in PFOA are bulkier and have a stronger bond to the electrons of the carbon chain than the hydrogens in octanoic acid (OA), the nonfluorinated molecule of similar structure.[6] This elemental change gives rise to structural differences between PFOA and OA; the alkyl chain of PFOA exhibits a helical conformation, rigid backbone, and low tendency of gauche defect formation when in monolayers.[16]

The environmental transport mechanisms of PFOA are via air and water. PFOA is a strong surfactant found in abundance at the air/water interface and the sea surface microlayer.[17,18] Thus, understanding the behavior of PFOA at the air/water interface is crucial for determining the fate and distribution of PFOAs in the environment.

Most environmental transport models analyzing the long-range dispersion of PFOA use the deprotonated form, PFO⁻, instead of PFOA.[17,19,20] This form is used because the PFOA is transported in water at neutral pH while PFOA is not protonated until at least pH 3.8.[21] However, the surface of water and submicron aerosols are more acidic than bulk water.[22,23] In addition to their pH dependence, the surface to volume ratio is higher for aerosols and submicrometer particles than other methods of environmental pollutant transport like rivers. Interactions between PFOA and sunlight or other chemicals can occur more readily on the surface of a submicrometer particle or aerosol. Several properties of the organic solutes, such as solubility, mixing transitions, and phase separation, can be impacted by the pH of a liquid and would differ between the surface and bulk molecules.[24] More information is needed to fill the knowledge gap about the pH-specific PFOA structure at the liquid−air interface.

The change in charged states, reactions, and properties of a molecule between the surface compared to the bulk means that pK_a cannot be obtained or calculated from bulk pK_a
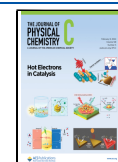
measurements alone. The surface pK_a is different from bulk pK_a, but it is vital for understanding how the state of the ions and charged acids or bases can impact the specific environments for organic lipids, proteins, and other molecules. This information directly correlates to a better understanding of the states of molecules found in biological membranes and performing biochemical functions or pollutants interacting with aerosols.[24,25] The surface pK_a has been measured with techniques that include zeta potential analysis, XPS, MD simulations, electronic and vibrational SFG, and surface tension.[26−33]

In this work, we determine the surface pK_a and surface structure of PFOA and OA at the air−water interface using sum frequency generation spectroscopy (SFG) and surface tension measurements. SFG spectroscopy is a second-order nonlinear technique. In vibrational SFG spectroscopy, an infrared beam is resonant with molecular vibrations and renders a vibrational spectrum of ordered molecules at the surface. Surface tension measurements analyze the capacity of the surfactants to disrupt the cohesive forces of the liquid molecules and can provide quantitative measurements of the surface pK_a.[31]

The pK_a of a surfactant gives crucial structural information, such as predicting in vivo function and activity of specific lipids.[34] SFG spectroscopy has been previously used to determine the surface pK_a and revealed the orientation and charge of various lengths of hydrocarbon carboxylic acids at the air/water surface.[35−37] Furthermore, SFG spectroscopy and surface tensiometry have been used to investigate the surface pK_a hydrocarbon carboxylic acids of various lengths at the air/water surface.[30−32] These complementary methods provide information about the PFOA and OA structural and charged states at the air−water interface.

2. EXPERIMENTAL METHODS

Perfluorooctanoic acid (PFOA, 95%), octanoic acid (OA, > 99%), and deuterium hydroxide (D_2O, 99.9 atom % D) were purchased from Sigma-Aldrich and used without further purification. For SFG samples, 1 mM solutions of PFOA and OA in D_2O were prepared by 40 °C sonicated bath then adjusted with sodium deuteroxide (NaOD, 40 wt % in D_2O) purchased from Acros Organics or deuterium chloride (DCl, 35 wt % in D_2O) purchased from Sigma-Aldrich Millipore to raise or lower the pH, respectively. For surface tension measurements, PFOA and OA were diluted to 1 mM with ultrapure water with 18.2 MΩ cm resistivity (Genpure Pro Water Purification System, Barnstead, Thermo Scientific) in a process similar to that before, but the pH was adjusted with hydrochloric acid (HCl, 37%) or sodium hydroxide (NaOH, 98%) from Sigma-Aldrich. The samples of 1 mM PFOA and OA were stored and pH adjusted at room temperature in 20 mL glass scintillation vials. Samples for SFG experiments were pipetted in 10 mL aliquots to pure Teflon dishes, while the surface tension experiments were conducted with 5 mL aliquots of sample in Teflon-coated aluminum dishes.

The S400-BIO SevenExcellence pH/mV meter from Mettler Toledo was calibrated and used to measure the pH of samples in H_2O. D_2O was the diluent for SFG samples to eliminate spectral interference in the water bending mode. For deuterated samples, the pD was calculated from the measured pH by

$$pD = pH + 0.44 \tag{1}$$

pH*, the pH equivalence of the acidity of the deuterated samples, was calculated by

$$pH^* = pD \times 0.929 \tag{2}$$

The sample titration range covered pH 0.5−8.0 since above pH 8, no significant changes were observed as the surface stayed dominated by the molecule's protonated form.

A DeltaPi surface tensiometer equipped with DyneProbes (Kibron, Finland) was used to measure the surface tension of the samples by the Wilhelmy method. Before samples, the surface tensiometer was calibrated with ultrapure water to 72.8 mN/m.[23] The samples were pipetted into the Teflon coated aluminum dish 20 min prior to surface tension measurements for the surfactants to reach equilibrium at the surface. The surface tension of each sample was taken after the reading remained constant for 2 min. Reported errors represent one standard deviation from the average of the triplicate measurements.

The sum frequency generation (SFG) measurements were performed on a vibrational SFG spectroscopy system utilizing a Ti:sapphire regenerative amplifier (Astrella, Coherent). The output of the Ti:sapphire regenerative amplifier is centered at 800 nm and consists of 5 mJ, ∼ 60 fs pulses with a 1 kHz repetition rate. The beam is split, and one portion is sent to a commercially available optical parametric amplifier (TOPAS Prime, Light Conversion) coupled with a DFG stage to generate tunable mid-IR, ∼9 μJ, light (ω_{IR}) centered at 6200 nm. The other portion of the beam passes through an interference filter (Andover) to frequency narrow the pulse bandwidth to 0.5 nm (fwhm ∼ 10 $cm^{−1}$) with a pulse energy of ∼20 μJ that will be used for the visible beam (ω_{vis}). Both beam paths then have a half-wave plate and a wire grid polarizer to control the polarization to be SSP (S-polarized SFG, S-polarized Vis, and P-polarized IR) or SPS (S-polarized SFG, P-polarized Vis, and S-polarized IR). To generate the SFG signal, the IR and visible light pulses are overlapped in time and space, and both beams focused onto the sample with a 300 mm focal length lens for the visible path and 100 mm focal length lens for the IR path. The IR and vis beams are directed to the sample at 35° and 60°, respectively, relative to surface normal. The SFG signal is collimated and subsequently detected by a spectrometer consisting of grating (1200 grooves/mm) and CCD camera (ISOPlane160 and Pixis400, Princeton Instruments). The SFG signal was acquired for 600 s for each sample. Background spectra were obtained by blocking the IR beam and subtracted from the sample signal. Reference SFG spectra using z-cut quartz were collected and used to normalize the sample data by dividing sample spectra by the reference spectrum.[38] The sample area and IR beam path were purged with dry air (CO_2 Absorber/Dryer, PUREGAS).

The observed spectra were fit to quantify the spectral changes between different pH* values by combining four Lorentzian functions and a nonresonant signal as given below:

$$I_{VSFG} \propto \left| A_{NR}\, e^{i\varphi_{NR}} + \frac{A_i}{\omega - \omega_i + i\Gamma_i} \right|^2 \tag{3}$$

The nonresonant contributions consist of an amplitude (A_{NR}) and phase (ϕ_{NR}) while the resonant components are the amplitude (A_i), central frequency (ω_i), and width (Γ_i) of the contributions from vibrational mode i.

3. RESULTS AND DISCUSSION

To assess the predominant species between protonated and deprotonated molecules at the surface, we first analyzed the
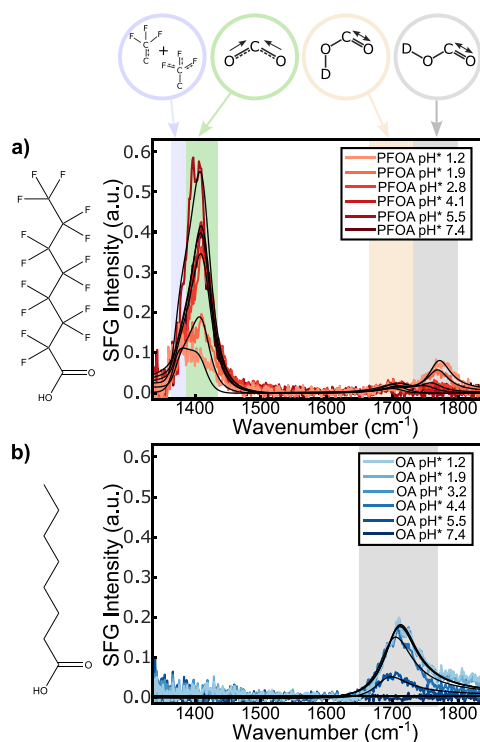
Figure 1. Molecular structure and SFG spectra of pH-adjusted samples of PFOA (a) and OA (b) from 1335 to 1835 cm^{-1} in SSP polarization. The SFG data were fit (black lines) with Lorentzian line shapes and identified with color-coded regions and visualization of the vibration.

Table 1. Fitting Parameters for the SFG Spectra of 1 mM OA in D$_2$O at Various pH*s in SSP Polarization with Gamma Reported in FWHM

pH*	A_R with A_{NR} = 0.02, φ_{NR} = −0.13, and Γ_i = 60 cm^{-1}	ω_i (cm^{-1})
1.2	13.5 ± 2.6	1710 ± 3
1.9	12.4 ± 0.4	1707 ± 0
3.2	12.7 ± 0.3	1707 ± 0
4.4	13.1 ± 1.9	1702 ± 3
5.5	7.0 ± 2.3	1693 ± 2
7.4	0	0

SFG spectra of the surfactants at different pHs and compared fluorinated PFOA to nonfluorinated OA. Figure 1 presents the

Figure 2. SFG spectra of 1 mM PFOA from 1585 to 1760 cm^{-1} in SPS polarization at pH* adjusted to 1.9 and 7.4. The peak areas of the asymmetric stretch of the deprotonated carboxylate anion (ν_{A,COO^-}) are identified with a blue shaded region, and the visualization of the vibration is in a circle above the spectra.
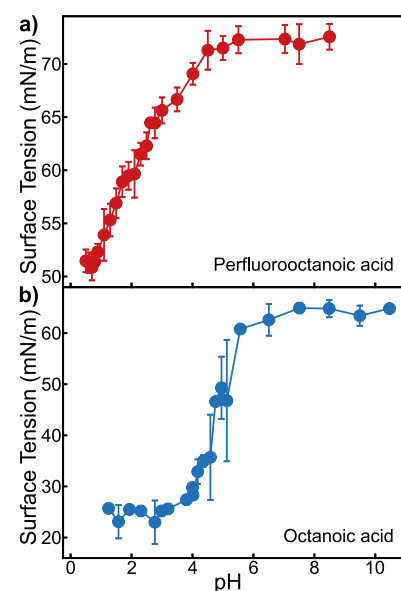
Figure 3. Surface tension vs pH titration curves for 1 mM PFOA (a) and OA (b) solutions with vertical error bars representing ± one standard deviation. Lines between data points are drawn to guide the eye.

molecular structures, SFG spectra, and fits for 1 mM PFOA (a) and OA (b) at the air−D$_2$O interface in the carbonyl frequency region 1335−1835 cm^{-1}. The corresponding SFG fits and

Table 2. Fitting Parameters for the SFG Spectra of 1 mM PFOA in D$_2$O at Various pH*s in SSP Polarization with Gamma Reported in FWHM

ω_i	1370 cm^{-1}	1412 cm^{-1}	1705 cm^{-1}	($\nu_{C=O}$)	
Γ_i	30	45	50	40	
pH*	A_R with A_{NR}= 0.07 and φ_{NR}= −0.2				$\nu_{C=O}$ ω_i (cm^{-1})
1.2	3.7 ± 0.5	−5.1 ± 0.3	−3.1 ± 0.8	4.4 ± 1.7	1768 ± 2
1.9	2.8 ± 0.5	−8.9 ± 1.4	−3.7 ± 0.6	4.5 ± 0.7	1766 ± 1
2.8	1.6 ± 0.2	−12.7 ± 2.2	−4.4 ± 0.2	3.9 ± 0.5	1762 ± 2
4.1	1.2 ± 0.3	−14.0 ± 1.2	−4.6 ± 0.2	3.1 ± 0.1	1758 ± 2
5.5	2.8 ± 0.9	−14.4 ± 0.9	−4.0 ± 0.8	0	0
7.4	1.2 ± 0.2	−13.2 ± 0.8	−3.9 ± 0.1	0	0
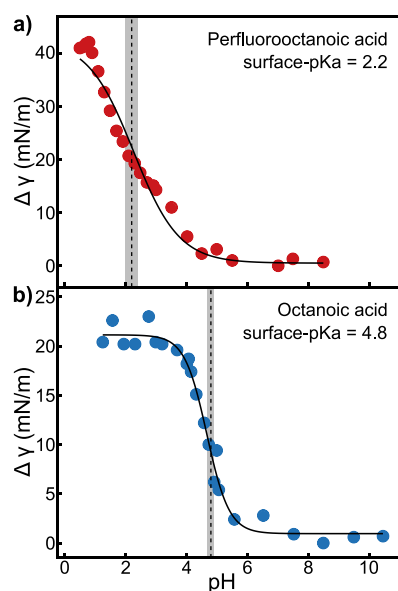
Figure 4. Surface activity models (solid black line) for PFOA (a) and OA (b) fit to the surface tension data transformed by $\Delta\gamma=\Delta\gamma_{max}-\gamma$. The average surface pK_as are denoted by vertical black dashed lines, while the surface pK_a errors representing one standard deviation are denoted by vertical gray shadows.

parameters for OA are listed in Table 1. The SFG spectrum of OA has one spectral feature around ∼1700 cm^{-1} attributed to the carbonyl stretch of the protonated carboxylic acid headgroup (ν_{COOD}).[39] The intensity of the 1700 cm^{-1} peak decreases with a blue shift as the pH increases, and the concentration of the acidic form of OA decreases.

The SFG spectrum of 1 mM PFOA, as shown in Figure 1a, has four spectral features in this region: 1370, 1412, 1705, and ∼1760 cm^{-1}. Table 2 presents the obtained parameters of the SFG fits for PFOA. The assignment of the peak at 1370 cm^{-1} to the coupling between the terminal C−C and C−F$_3$ bonds of the PFOA alkyl chain is based on studies using heterodyne SFG spectroscopy.[40,41] The 1412 and 1760 cm^{-1} peaks are inversely related as the pH is adjusted. At high pH, the dominant signal is at 1412 cm^{-1} and is attributed to the symmetric stretch of the carboxylate headgroup ($\nu_{SS,COO-}$).[42] As the pH decreases, two peaks emerge at 1705 and 1760 cm^{-1}. The 1705 cm^{-1} peak may be attributed to coupling between the deprotonated and protonated forms, while 1760 cm^{-1} corresponds to the carbonyl stretch of the carboxylic acid groups ($\nu_{C=O}$).[43] Another assignment of these peaks based on a 2D-IR study determined the spectral features are due to the different positions of the hydroxyl (O−D) group in relation to the carbonyl group: 1705 cm^{-1} for the syn-conformation and 1760 cm^{-1} for the anticonformation.[44,45] The assignment of the symmetric stretch of the deprotonated headgroup and the carbonyl stretch from the protonated headgroup is consistent with other SFG studies on short- or long-chain carboxylic acids and amino acids.[46]

SFG spectra were collected in the SPS polarization combination to investigate the peak assignment possibilities at 1705 cm^{-1} in SSP polarization. There is one peak visible for PFOA between 1585 and 1760 cm^{-1} in the SPS polarization, as illustrated in Figure 2, at 1675 cm^{-1} assigned to the asymmetric stretch of the carboxylate anion ($\nu_{A,COO-}$) due to its appearance at higher pHs and classification in other studies.[41] In these other studies, the asymmetric stretch peak in

SPS polarization has been used to calculate the twist and tilt angle of the surface PFOA.[42,45] Based on the peaks present in the SSP and SPS polarizations, all oxygens are below the liquid's surface, the surfactants are well-ordered and packed, and the terminal C−C bond is perpendicular to the surface with the three fluorines bound to it are facing up and away from the surface.[45,46] Since the structural peak at 1370 cm^{-1} did not significantly change and no other peaks appeared, the orientation and packing described are maintained at each pH analyzed.

SFG signal intensity depends on the bond population at the surface and the orientation related to the polarization.[47] The PFOA tail-specific peak at 1370 cm^{-1} in SSP does not significantly change between the different pH values. Thus, the data indicate that the total population, packing, and orientation of the molecules at the air/water interface are not changing. The peaks that change with pH in either polarization or molecule are part of the acidic headgroup. As shown in Tables 1 and 2, the signal for the carbonyl stretching vibration disappeared entirely for both OA and PFOA. The disappearance of these peaks is consistent with the bulk pK_a trends of the molecules. PFOA has a lower bulk pK_a than OA.

Some studies have compared the pH-dependent peak areas of the SFG signal from protonated and deprotonated headgroup vibrations to calculate the pK_a. It appears that the dissociation occurs between pH* 1.9 and pH* 4.1, but this method is not ideal for these compounds. Calculating the pK_a in this method is generally used to compare the surface pK_a to the bulk pK_a.[30,32] There are two main reasons that this method was not performed for these spectra. First, OA only has one pH-dependent peak in this region, so this method could not be employed. Second, the PFOA peak at 1370 cm^{-1} may interfere with the deprotonated headgroup associated peak at 1412 cm^{-1} that would be compared to the protonated headgroup associated peak. Interference of the 1370 and 1412 cm^{-1} peaks could prevent optimal peak fitting and data interpretation. While this method of further SFG analysis is rigorous, it is not ideal for these chemicals of interest, and a secondary method is utilized.

Figure 3 shows the surface tensions of 1 mM PFOA (a) and OA (b) over a wide range of pH values. This surface tension method provides quantitative surface pK_a for PFOA and OA. The surface tension data are transformed into a surface activity model, shown in Figure 4, by subtracting the surface tension at each pH, $\Delta\gamma$ from the maximum surface tension, $\Delta\gamma_{max}$. The surface activity models of PFOA and OA were fit with a sigmoidal curve to calculate the pH at which dissociation occurs.[31] The surface pK_a is significantly different at the surface than in the bulk environment for PFOA: 2.2 for the surface pK_a and between 0 and 3.8 for the reported bulk pK_a.[13,14] This is unique to the fluorinated form because the surface and reported bulk dissociation values of OA are 4.9.[14] Interfacial PFOA has a higher degree of packing at the surface than OA due to the helical structure of the PFOA fluorocarbon alkyl chain.[16,33,48]

The methodology used here is both well-established to determine the surface pK_a of surface-active species. Despite the disparity in the literature-reported bulk pK_a values, these two very different techniques were in agreement with producing the surface specific pK_a from a one-to-one correspondence between the apparent point of dissociation from SFG spectra and the calculated value from surface tensiometry.

4. CONCLUSIONS

We investigated the surface pK_a by analyzing PFOA and OA over a range of pH values with SFG spectroscopy in the carbonyl region from 1300 to 1800 cm^{-1} and surface tensiometry. The amplitudes of the PFOA carbonyl and carboxylate anion vibrations directly depended on the pH of the sample analyzed. The reduction and disappearance of the symmetric carbonyl stretch peak occur at a lower pH in PFOA than in OA, which is consistent with the bulk pK_a of OA being greater than the reported values of bulk pK_a for PFOA. The surface tension measurements provide the quantitative pH at which the respective acids dissociate at the air/water interface. The surface pK_a calculated by fitting the surface activity of OA, 4.8 ± 0.1, does not differ from its bulk reported values. However, the calculated surface pK_a for PFOA is 2.2 ± 0.2, significantly lower than some of the reported bulk pK_a values for PFOA. This understanding could give more details for the long-form atmospheric transport models and provide a better understanding of the environmental impact of PFOA and other PFAS.

■ AUTHOR INFORMATION

Corresponding Author

    Jenée D. Cyran − *Boise State University, Boise, Idaho 83725, United States of America*; Email: jeneecyran@boisestate.edu

Authors

    Lila J. Musegades − *Baylor University, Waco, Texas 76798, United States of America*

    Owen P. Curtin − *Boise State University, Boise, Idaho 83725, United States of America*

Complete contact information is available at:
https://pubs.acs.org/10.1021/acs.jpcc.3c07235

Notes

The authors declare no competing financial interest.

■ ACKNOWLEDGMENTS

■ REFERENCES

(1) Goosey, E.; Harrad, S. Perfluoroalkyl Compounds in Dust from Asian, Australian, European, and North American Homes and UK Cars, Classrooms, and Offices. *Environ. Int.* **2011**, *37*, 86−92.

(2) Hu, X. C.; Andrews, D. Q.; Lindstrom, A. B.; Bruton, T. A.; Schaider, L. A.; Grandjean, P.; Lohmann, R.; Carignan, C. C.; Blum, A.; Balan, S. A.; et al. Detection of Poly- and Perfluoroalkyl Substances (PFASs) in U.S. Drinking Water Linked to Industrial Sites, Military Fire Training Areas, and Wastewater Treatment Plants. *Environ. Sci. Technol. Lett.* **2016**, *3*, 344−350.

(3) Krafft, M. P.; Riess, J. G. Therapeutic Oxygen Delivery by Perfluorocarbon-Based Colloids. *Adv. Colloid Interface Sci.* **2021**, *294*, 102407.

(4) Abadian, H.; El-Yahklifi, S.; Ayela, B.; Felder-Flesch, D.; Schmutz, M.; Krafft, M. P. Activatable Perfluorocarbon Nano-emulsions Stabilized by Oligo(Ethylene Glycol) Bisphosphonate Dendrons: Methods of Preparation and Characterization. *J. Acoust. Soc. Am.* **2022**, *152*, A77−A77.

(5) Schwartz-Narbonne, H.; Xia, C.; Shalin, A.; Whitehead, H. D.; Yang, D.; Peaslee, G. F.; Wang, Z.; Wu, Y.; Peng, H.; Blum, A.; et al.

Per- and Polyfluoroalkyl Substances in Canadian Fast Food Packaging. *Environ. Sci. Technol. Lett.* **2023**, *10*, 343−349.

(6) Riess, J. G. Understanding the Fundamentals of Perfluor-ocarbons and Perfluorocarbon Emulsions Relevant to *In Vivo* Oxygen Delivery. *Artif. Cells, Blood Substitutes, Biotechnol.* **2005**, *33*, 47−63.

(7) Cousins, I. T.; Dewitt, J. C.; Glüge, J.; Goldenman, G.; Herzke, D.; Lohmann, R.; Ng, C. A.; Scheringer, M.; Wang, Z. The High Persistence of PFAS Is Sufficient for Their Management as a Chemical Class. *Environ. Sci.: processes Impacts* **2020**, *22*, 2307−2312.

(8) Olsen, G. W.; Burris, J. M.; Ehresman, D. J.; Froehlich, J. W.; Seacat, A. M.; Butenhoff, J. L.; Zobel, L. R. Half-Life of Serum Elimination of Perfluorooctanesulfonate,Perfluorohexanesulfonate, and Perfluorooctanoate in Retired Fluorochemical Production Workers. *Environ. Health Perspect.* **2007**, *115*, 1298−1305.

(9) Jing, P.; Rodgers, P. J.; Amemiya, S. High Lipophilicity of Perfluoroalkyl Carboxylate and Sulfonate: Implications for Their Membrane Permeability. *J. Am. Chem. Soc.* **2009**, *131*, 2290−2296.

(10) Melzer, D.; Rice, N.; Depledge, M. H.; Henley, W. E.; Galloway, T. S. Association between Serum Perfluorooctanoic Acid (PFOA) and Thyroid Disease in the U.S. National Health and Nutrition Examination Survey. *Environ. Health Perspect.* **2010**, *118*, 686−692.

(11) Rickard, B. P.; Rizvi, I.; Fenton, S. E. Per- and Poly-Fluoroalkyl Substances (PFAS) and Female Reproductive Outcomes: PFAS Elimination, Endocrine-Mediated Effects, and Disease. *Toxicology* **2022**, *465*, 153031.

(12) Li, K.; Gao, P.; Xiang, P.; Zhang, X.; Cui, X.; Ma, L. Q. Molecular Mechanisms of PFOA-Induced Toxicity in Animals and Humans: Implications for Health Risks. *Environ. Int.* **2017**, *99*, 43−54.

(13) Goss, K.-U. The pK_a Values of PFOA and Other Highly Fluorinated Carboxylic Acids. *Environ. Sci. Technol.* **2008**, *42*, 456−458.

(14) Burns, D. C.; Ellis, D. A.; Li, H.; McMurdo, C. J.; Webster, E. Experimental pK_a Determination for Perfluorooctanoic Acid (PFOA) and the Potential Impact of pK_a Concentration Dependence on Laboratory-Measured Partitioning Phenomena and Environmental Modeling. *Environ. Sci. Technol.* **2008**, *42*, 9283−9288.

(15) Moroi, Y.; Yano, H.; Shibata, O.; Yonemitsu, T. Determination of Acidity Constants of Perfluoroalkanoic Acids. *Bull. Chem. Soc. Jpn.* **2001**, *74*, 667−672.

(16) Bunn, C. W.; Howells, E. R. Structures of Molecules and Crystals of Fluoro-Carbons. *Nature* **1954**, *174*, 549−551.

(17) Psillakis, E.; Cheng, J.; Hoffmann, M. R.; Colussi, A. J. Enrichment Factors of Perfluoroalkyl Oxoanions at the Air/Water Interface. *J. Phys. Chem. A* **2009**, *113*, 8826−8829.

(18) Ju, X.; Jin, Y.; Sasaki, K.; Saito, N. Perfluorinated Surfactants in Surface, Subsurface Water and Microlayer from Dalian Coastal Waters in China. *Environ. Sci. Technol.* **2008**, *42*, 3538−3542.

(19) Lyu, Y.; Brusseau, M. L.; Chen, W.; Yan, N.; Fu, X.; Lin, X. Adsorption of PFOA at the Air−Water Interface during Transport in Unsaturated Porous Media. *Environ. Sci. Technol.* **2018**, *52*, 7745−7753.

(20) Rayne, S.; Forest, K. Theoretical Studies on the pK ∼ a∼ Values of Perfluoroalkyl Carboxylic Acids. *Nat. Preced.* **2010**, *11*. .

(21) Webster, E.; Ellis, D. A.; Reid, L. K. Modeling the Environmental Fate of Perfluorooctanoic Acid and Perfluoroocta-noate: An Investigation of the Role of Individual Species Partitioning. *Environ. Toxicol. Chem.* **2010**, *29*, 1466−1475.

(22) Angle, K. J.; Crocker, D. R.; Simpson, R. M. C.; Mayer, K. J.; Garofalo, L. A.; Moore, A. N.; Or, V. W.; Srinivasan, S.; Farhan, M.; et al. Acidity across the Interface from the Ocean Surface to Sea Spray Aerosol. *Proc. Natl. Acad. Sci. U. S. A.* **2021**, *118*, No. e2018397118.

(23) Buch, V.; Milet, A.; Vácha, R.; Jungwirth, P.; Devlin, J. P. Water Surface Is Acidic. *Proc. Natl. Acad. Sci. U. S. A.* **2007**, *104*, 7342−7347.

(24) Losey, D. J.; Parker, R. G.; Freedman, M. A. pH Dependence of Liquid−Liquid Phase Separation in Organic Aerosol. *J. Phys. Chem. Lett.* **2016**, *7*, 3861−3865.

(25) Panahi, A.; Brooks, C. L. Membrane Environment Modulates the p K_a Values of Transmembrane Helices. *J. Phys. Chem. B* **2015**, *119*, 4601−4607.

(26) Quast, K. The Use of Zeta Potential to Investigate the p K_a of Saturated Fatty Acids. *Adv. Powder Technol.* **2016**, *27*, 207−214.

(27) Vysotsky, Y. B.; Kartashynska, E. S.; Vollhardt, D.; Fainerman, V. B. Surface p K_a of Saturated Carboxylic Acids at the Air/Water Interface: A Quantum Chemical Approach. *J. Phys. Chem. C* **2020**, *124*, 13809−13818.

(28) Werner, J.; Persson, I.; Björneholm, O.; Kawecki, D.; Saak, C.-M.; Walz, M.-M.; Ekholm, V.; Unger, I.; Valtl, C.; Caleman, C.; Öhrwall, G.; Prisle, N. L. Shifted Equilibria of Organic Acids and Bases in the Aqueous Surface Region. *Phys. Chem. Chem. Phys.* **2018**, *20*, 23281−23293.

(29) Kundu, A.; Yamaguchi, S.; Tahara, T. Evaluation of pH at Charged Lipid/Water Interfaces by Heterodyne-Detected Electronic Sum Frequency Generation. *J. Phys. Chem. Lett.* **2014**, *5*, 762−766.

(30) Lesnicki, D.; Wank, V. D.; Cyran, J. D.; Backus, E. H. G.; Sulpizi, M. Lower Degree of Dissociation of Pyruvic Acid at Water Surfaces than in Bulk. *Phys. Chem. Chem. Phys.* **2022**, *24*, 13510−13513.

(31) Wellen, B. A.; Lach, E. A.; Allen, H. C. Surface pKa of Octanoic, Nonanoic, and Decanoic Fatty Acids at the Air-Water Interface: Applications to Atmospheric Aerosol Chemistry. *Phys. Chem. Chem. Phys.* **2017**, *19*, 26551−26558.

(32) Strazdaite, S.; Meister, K.; Bakker, H. J. Reduced Acid Dissociation of Amino-Acids at the Surface of Water. *J. Am. Chem. Soc.* **2017**, *139*, 3716−3720.

(33) Zhang, T.; Brantley, S. L.; Verreault, D.; Dhankani, R.; Corcelli, S. A.; Allen, H. C. Effect of pH and Salt on Surface p K_a of Phosphatidic Acid Monolayers. *Langmuir* **2018**, *34*, 530−539.

(34) Alabi, C. A.; Love, K. T.; Sahay, G.; Yin, H.; Luly, K. M.; Langer, R.; Anderson, D. G. Multiparametric Approach for the Evaluation of Lipid Nanoparticles for siRNA Delivery. *Proc. Natl. Acad. Sci. U. S. A.* **2013**, *110*, 12881−12886.

(35) Tyrode, E.; Hedberg, J. A Comparative Study of the CD and CH Stretching Spectral Regions of Typical Surfactants Systems Using VSFS: Orientation Analysis of the Terminal CH_3 and CD_3 Groups. *J. Phys. Chem. C* **2012**, *116*, 1080−1091.

(36) Tyrode, E.; Corkery, R. Charging of Carboxylic Acid Monolayers with Monovalent Ions at Low Ionic Strengths: Molecular Insight Revealed by Vibrational Sum Frequency Spectroscopy. *J. Phys. Chem. C* **2018**, *122*, 28775−28786.

(37) Moll, C. J.; Versluis, J.; Bakker, H. J. Bulk Response of Carboxylic Acid Solutions Observed with Surface Sum-Frequency Generation Spectroscopy. *J. Phys. Chem. B* **2022**, *126*, 270−277.

(38) Bain, C. D.; Davies, P. B.; Ong, T. H.; Ward, R. N.; Brown, M. A. Quantitative Analysis of Monolayer Composition by Sum-Frequency Vibrational Spectroscopy. *Langmuir* **1991**, *7*, 1563−1566.

(39) Dreier, L. B.; Bonn, M.; Backus, E. H. G. Hydration and Orientation of Carbonyl Groups in Oppositely Charged Lipid Monolayers on Water. *J. Phys. Chem. B* **2019**, *123*, 1085−1089.

(40) Okuno, M.; Homma, O.; Kuo, A.-T.; Urata, S.; Koguchi, R.; Miyajima, T.; Ishibashi, T. Molecular Orientations and Conformations of Air/Fluoroalkyl Acrylate Polymer Interfaces Studied by Heterodyne-Detected Vibrational Sum Frequency Generation. *Macromolecules* **2019**, *52*, 8705−8712.

(41) Tyrode, E.; Johnson, C. M.; Rutland, M. W.; Day, J. P. R.; Bain, C. D. A Study of the Adsorption of Ammonium Perfluorononanoate at the Air−Liquid Interface by Vibrational Sum-Frequency Spectroscopy. *J. Phys. Chem. C* **2007**, *111*, 316−329.

(42) Korotkevich, A. A.; Moll, C. J.; Versluis, J.; Bakker, H. J. Molecular Orientation of Carboxylate Anions at the Water−Air Interface Studied with Heterodyne-Detected Vibrational Sum-Frequency Generation. *J. Phys. Chem. B* **2023**, *127*, 4544−4553.

(43) Vaillard, A.-S.; El Haitami, A.; Dreier, L. B.; Fontaine, P.; Cousin, F.; Gutfreund, P.; Goldmann, M.; Backus, E. H. G.; Cantin, S. Vertically Heterogeneous 2D Semi-Interpenetrating Networks Based on Cellulose Acetate and Cross-Linked Polybutadiene. *Langmuir* **2022**, *38*, 2538−2549.

(44) Giubertoni, G.; Sofronov, O. O.; Bakker, H. J. Observation of Distinct Carboxylic Acid Conformers in Aqueous Solution. *J. Phys. Chem. Lett.* **2019**, *10*, 3217−3222.

(45) Yu, C.-C.; Imoto, S.; Seki, T.; Chiang, K.-Y.; Sun, S.; Bonn, M.; Nagata, Y. Accurate Molecular Orientation at Interfaces Determined by Multimode Polarization-Dependent Heterodyne-Detected Sum-Frequency Generation Spectroscopy via Multidimensional Orientational Distribution Function. *J. Chem. Phys.* **2022**, *156*, 094703.

(46) Moll, C. J.; Korotkevich, A. A.; Versluis, J.; Bakker, H. J. Molecular Orientation of Small Carboxylates at the Water−Air Interface. *Phys. Chem. Chem. Phys.* **2022**, *24*, 10134−10139.

(47) Sthoer, A.; Hladílková, J.; Lund, M.; Tyrode, E. Molecular Insight into Carboxylic Acid−Alkali Metal Cations Interactions: Reversed Affinities and Ion-Pair Formation Revealed by Non-Linear Optics and Simulations. *Phys. Chem. Chem. Phys.* **2019**, *21*, 11329−11344.

(48) Krafft, M. Monolayers Made from Fluorinated Amphiphiles. *Curr. Opin. Colloid. Interface Sci.* **2003**, *8*, 243−250.